Photochemistry and Photobiology, 2011, 87: 1395–1404

A Nonionic Porphyrin as a Noninterfering DNA Antibacterial Agent

Sónia Mendes[1], Fábio Camacho[1], Tito Silva[1], Cecília R. C. Calado[1], Arménio Coimbra Serra*[2], António M. d'A. Rocha Gonsalves[2] and Mónica Roxo-Rosa*[1]

[1]Faculdade de Engenharia, Universidade Católica Portuguesa, Rio de Mouro, Portugal
[2]Chymiotechnon, Departamento de Química, Universidade de Coimbra, Coimbra, Portugal

Received 3 May 2011, accepted 1 August 2011, DOI: 10.1111/j.1751-1097.2011.00984.x

ABSTRACT

The increasing interest in clinical bacterial photodynamic inactivation has led to the search for photosensitizers with higher bactericidal efficiency and less side effects on the surrounding tissues. We present a novel nonionic porphyrin, the 5,10,15-tris(2,6-dichlorophenyl)-20-[4-*N*-(6-amino-hexyl)sulfonamido)phenyl]-porphyrin (ACS769F4) with substantial improvements in the efficiency of nonionic sensitizers. This porphyrin causes eradication of both *Escherichia coli* and *Staphylococcus aureus* by the photodynamic effect but in higher concentrations compared with 5,10,15,20-tetrakis (4-*N*,*N*,*N*-trimethylammoniumphenyl)-porphyrin *p*-tosylate ($TTAP^{4+}$), a known bactericidal tetracationic porphyrin. More important, under such conditions, ACS769F4 proved to be harmless to two mammalian cells lines (human embryonic and baby hamster kidney), causing no reduction in their viability or negative impact on their cytoskeleton, despite its accumulation in cellular structures. On the contrary, $TTAP^{4+}$ is shown to accumulate in the nucleus of mammalian cells, in association to DNA, causing chromatin condensation after exposure to light. Furthermore, dark incubation with $TTAP^{4+}$ was shown to have a deleterious effect on the microtubule network. Based on its bactericidal efficiency, also observed without exposure to light, and on the low tendency to be harmful or genotoxic to mammalian cells, ACS769F4 should be looked at as an interesting photosensitizer to be evaluated for clinical purposes.

INTRODUCTION

The use of light as a therapeutic tool, known in ancient Greece, Egypt and India and forgotten for centuries, was rediscovered in the early 20th century. The clinical method now known as photodynamic therapy (PDT), is based on using a nontoxic photosensitive molecule that once activated by visible light, triggers a destructive action in biological systems due to the generation of cytotoxic oxygen species of the radical type (Type I reactions) or singlet oxygen ($^1O_2$) (Type II reactions) (1). Due to their short lifetimes and diffusion paths, these highly reactive species interact with biomolecules in their immediate vicinity leading to severe cell damage (1).

In many countries, PDT has regulatory approval for treatment of several malignant and nonmalignant diseases. The application of PDT in *in vitro* inactivation of viruses (2), bacteria (3), fungi (4) and protozoa (5) has also been shown to be effective. The interest in PDT bactericidal effect increased in the last decade strongly reinforced by the worldwide rise in antibiotic resistance (3). Data from multiple treatments suggest that bacterial photodynamic inactivation (PDI) is unlikely to induce bacterial resistance (3,6) and that its efficiency is independent of the pattern of antibiotic resistance of the strain (7). With its broad spectrum of action (8), PDI has shown promising results in treating animal models (9) and human infections. Indeed, PDI seems efficient in eradicating *Helicobacter pylori* from its natural niche, the human stomach, in a small group of infected patients (10). It was also shown to be a better approach than the standard endodontic treatment in the elimination of bacterial biofilms in root canals (11). Even better results were obtained by combining these two therapies (11), a procedure that is already in clinical trials (12).

Gram-positive strains are generally sensitive to PDI (8). On the contrary, Gram-negative bacteria, with their additional lipid membrane, located externally to the peptidoglycan network, strongly impairing the electrostatic attraction to negatively and noncharged sensitizers, are not efficiently inactivated (8). This can be overcome using permeabilization agents or cationic porphyrins (13–17), as for example 5,10,15,20-tetrakis(4-*N*,*N*,*N*-trimethylammoniumphenyl)-porphyrin *p*-tosylate ($TTAP^{4+}$), a frequently used and active sensitizer established to eradicate *Escherichia coli* (14,18). Recently, research has focused on the study of structural features of sensitizers that somehow potentiate their antimicrobial effects. In fact, properties such as the number and type of charge, its distribution over the molecule and the presence of long hydrocarbon chains, have an influence on the hydrophilicity of the sensitizer and therefore, on its cellular distribution and its effectiveness (19). For treatment of infections and notwithstanding the bactericidal potential of sensitizers, their interaction with surrounding healthy tissues should be considered. Therefore, the intracellular distribution of sensitizers in mammalian cells should be evaluated. It is known that accumulation of a sensitizer in the nucleus of cells increases the risk of DNA damage, mutations and carcinogenesis, while its accumulation in mitochondria is likely to

*Corresponding author email: armenio.serra@gmail.com (Arménio Serra); mroxorosa@fe.lisboa.ucp.pt (Mónica Roxo-Rosa)

induce apoptosis. Moreover, their accumulation in lysosomes or endosomes leads to permeabilization of these organelles, with the consequent release of the sensitizer to the cytosol, where it can sensitize tubulin to photodamage (20).

The present study focuses on the evaluation of the bactericidal efficiency of a novel neutral porphyrin, 5,10,15-tris(2,6-dichlorophenyl)-20-[4-*N*-(6-amino-hexyl)sulfonamido phenyl] porphyrin (ACS769F4), in inactivation of *Staphylococcus aureus* and *E. coli*. Furthermore, the potential impact of this molecule on human tissue was assessed by characterizing the events that occur in mammalian cells treated with ACS769F4 in the dark and after photosensitization. These results were compared with those obtained using $TTAP^{4+}$.

MATERIALS AND METHODS

Synthesis and characterization of ACS769F4 porphyrin. At room temperature, 20 mL of chlorosulfonic acid were added to 650 mg of a mixture of porphyrins 1 and 2, in a ratio of 13–72% prepared as previously described (21) (Fig. 1). After stirring for 2 h, the chlorosulfonyl derivative 3 and the unreacted porphyrin 1 were precipitated by pouring the solution carefully over ice. The precipitate was filtered, dried, dissolved with dichloromethane and the solution dried with sodium sulfate (Na_2SO_4). The solution was concentrated to 30 mL and 1,6-hexanediamine (4 g) and pyridine (10 mL) were added. The mixture was stirred overnight at 30°C, filtered, washed with water, dried with Na_2SO_4 and chromatographed on silica gel type 60 (particle size of 0.035–0.070 μm; Acros Organics). The porphyrin fraction was eluted using dichlorometane with increasing amounts of ethanol up to 40%. Evaporation of the solvent gave 120 mg of pure ACS769F4 (Fig. 1), as a purple powder. ^{1}H NMR (300 MHz, $CDCl_3$) δ_H = 1.4–1.7 (m), 3.3 (bs), 7.9 (m), 8.4 (m), 8.8 (m) (300 MHz Bruker-AMX spectrometer, *J* values are given in Hz), MS (ESI): *m/z* = 999 ($[M + 1]^+$, 100%) (Finnigan Advantage spectrometer), $C_{50}H_{38}Cl_6N_6O_6S.2H_2O$: Calcd. C, 58.0; H, 4.09; N, 8.11. Found: C, 58.3; H, 3.73; N, 7.63% (EA1108-CHNS-0 elemental analyser; Fisons Instruments). UV–Vis spectra (CH_2Cl_2), $\lambda_{máx}$ (nm): 418, 512, 587.5, 648 (U-2001 spectrophotometer; Hitachi) (see Figures S1–S4 for characterization).

$TTAP^{4+}$ was purchased from Sigma-Aldrich (Sigma-Aldrich Company, St. Louis, MO) (molecular mass: 1531.9 Da).

Both sensitizers were stored protected from light, at room temperature, as 500 μM stock solutions in 2.5% (vol/vol) dimethylformamide (DMF) (Sigma-Aldrich) and diluted in ultrapure water for the following experiments.

Light source and irradiation setup. The light source was a 300 W halogen lamp (Haloline^{-} lamp; OSRAM, Germany) (emission wavelength 350–950 nm), positioned 42 cm above samples, delivering a fluence rate of 9.35 mW cm^{-2} (X97 radiometer; Gigahertz-Optik). Room temperature was insured by using a thermostatic circulatory system (MultiTemp^{TM} III; GE Healthcare, UK) and by installing the irradiation setup inside a safety cabinet for bacterial and mammalian cell experiments, respectively.

Sensitizers' photobleaching. UV–Visible absorption spectra (350–650 nm) of 15 μM sensitizer solutions, before and during irradiation, were recorded and processed with a multi detection microplate reader (Synergy^{TM} 2; BioTek Instruments, Inc., Vermont) and the software GEN5^{TM} (BioTek Instruments, Inc.). Photobleaching kinetics were evaluated by following the absorbance (*A*) decrease at the Soret band wavelength (*ca* 420 nm) throughout irradiation. Photobleaching rate constants (*k*) were obtained by a linear least squares fit of the following semilogarithmic plot: natural logarithm of the ratio between the optical density (O.D.) (at 422 nm for ACS769F4 and 412 nm for $TTAP^{4+}$) at the beginning of the experiment (t = 0 min) (A_0) and the O.D. at a given time (A) [$\ln(A_0/A)$] *versus* irradiation time (t, min).

Cell culture conditions. *E. coli* (ATCC 25922) and *S. aureus* (ATCC 25923) bacterial cells were grown aerobically at 37°C, 220 rpm, in a complex growth medium (glucose 0.05% [wt/vol], yeast extract 0.2% [wt/vol], bactotryptone 0.1% [wt/vol], phosphate buffer at pH 7.0, all reagents purchased from Difco). BHK-21 (baby hamster kidney-21) and HEK (human embryonic kidney) cell lines were grown at 37°C with 5% CO_2 and 99% humidity in Dulbecco's modified Eagle's medium (DMEM/F12) (Invitrogen, Life Technologies, Carlsbad, CA) supplemented with 10% (vol/vol) fetal bovine serum (Invitrogen) and 1% (vol/vol) penicillin and streptomycin (Invitrogen).

Phototoxicity assays on bacteria. Fresh bacterial cell cultures were grown up to a cell density of 10^8 cells mL^{-1} (0.6 O.D. at 600 nm for *E. coli* or 0.8 for *S. aureus*), washed twice with cold PBS and resuspended in PBS at the same cell density. Cells were then incubated in the dark with different concentrations (1, 5, 10 and 15 μM) of ACS769F4 or $TTAP^{4+}$, for 30 min at 37°C and immediately irradiated for 15 min (light dose 8.4 J cm^{-2}). Control experiments: without irradiation in the presence of sensitizers; with and without irradiation in the absence of sensitizers; with DMF excluding porphyrins. Cell samples were then serially diluted 10-fold in PBS, in order to obtain dilutions of 10^{-1}–10^{-6} times of the initial concentration and 50 μL of

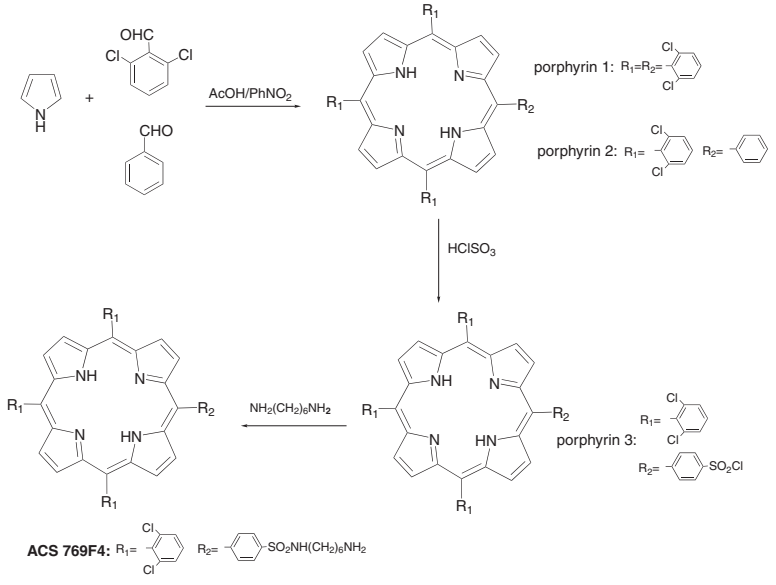

Figure 1. Sequence of reactions for the synthesis of the porphyrin ACS769F4.

each dilution were spread on agar plates (in triplicates) and incubated for 16 h at 37°C. Bacteria viability was then monitored by counting the CFUs and determining the survival fraction compared to the untreated control. Effective killing was taken to be >99.9% which corresponds to a reduction of 3 $\log_{10}$ in the survival fraction.

Phototoxicity assays on mammalian cells. BHK-21 and HEK cells grown in 24 multiwell plates (Nalge Nunc, Roskilde, Denmark) until 60–70% confluence and rinsed twice with cold PBS, were incubated with different concentrations up to 20 μM of ACS769F4 or $TTAP^{4+}$ for 30 min, in the dark, at 37°C. Cells were then irradiated for 40 min (light dose 22.4 J cm^{-2}). Control experiments: without irradiation in the presence of sensitizers; irradiation in the absence of sensitizers; DMF excluding porphyrins. Cell viability was assessed, immediately after light exposure, by a standard MTT assay. For normalization the value of 100 corresponds to cell viability without treatment with sensitizers and without light exposure.

Cellular localization. Cells from fresh cultures grown up to an O.D. (at 600 nm) of 2.0 for *E. coli* and of 4.0 for *S. aureus* were washed twice with cold PBS and were incubated with 10 μM of ACS769F4 or 5 μM $TTAP^{4+}$ in PBS, for 1 h in the dark. Then 4 μL of each cellular suspension were spread on a slide, dried and fixed by passing the slide through a flame.

BHK-21 cells grown on eight well chamber slides (Nalge Nunc), until 60–70% confluence were dark incubated with 10 μM of ACS769F4 or $TTAP^{4+}$ for 5 min, 1 h and 12 h at 37°C. After two washes with cold PBS, cells were fixed for 30 min at 4°C in 4% (vol/vol) formaldehyde (Sigma-Aldrich) and 3.7% (wt/vol) sucrose (Merck, Darmstadt, Germany) solution, in PBS.

Both bacterial and BHK-21 cell slides were mounted in Vectashield (Vector Laboratories, Burlingame, CA), containing DAPI (4,6-diamino-2-phenylindole) (Sigma-Aldrich) for nucleic acid staining whenever necessary. Sensitizers' fluorescence was observed and recorded on an Axiovert 40CFL fluorescence microscope (Carl Zeiss, Jena, Germany) equipped with the dual-band filter set-05 (excitation 395–440 nm; detection 470–850 nm; Carl Zeiss) and with an Axiocam MRc5 (Carl Zeiss) camera. Images were processed with the software AxioVision Rel. 4.6.3 (Carl Zeiss).

Immunocytochemistry analysis. BHK-21 cells grown on eight well chamber slides were dark incubated with 10 μM of ACS769F4 or 10 μM of $TTAP^{4+}$ for 1 h at 37°C. Cells were rinsed and fixed as above. After two washes with PBS, cells were permeabilized for 15 min with 0.2% (vol/vol) TritonX-100 (Sigma-Aldrich) in PBS at RT, then washed three more times with PBS and blocked with 1% (wt/vol) bovine serum albumin (BSA) in PBS for 30 min prior to incubation for 90 min at RT with the organelles' specific monoclonal antibodies (mAb) (1:1000 diluted in 0.5% [wt/vol] BSA in PBS). Primary mAbs: anti-Rab7 (clone Rab7-117) mAb (Sigma-Aldrich); anti-Golgi 58K protein/formimino-transferase cyclodeaminase (clone 58K-9) mAb (Sigma-Aldrich); anti-α-tubulin (clone DM1A) mAb (Sigma-Aldrich); antiactin (clone AC40) mAb (Sigma-Aldrich). Cells were then washed three times with PBS and incubated with the fluorescein isothiocyanate-conjugated antimouse IgG (Sigma-Aldrich) diluted at 1:100 for 30 min at RT and washed twice again. Immunofluorescence was observed as above, now using the filter set-10 (excitation 450–490 nm; detection 515–565 nm; Carl Zeiss) for detection of fluorescein alone or the filter set-05 for simultaneous detection of sensitizer and fluorescein.

Statistics. Results are expressed as means ± standard deviations (SD) of n observations. Differences were tested by Student's t-test, being considered as statistically significant when $P < 0.05$. Each experiment was performed at least in triplicate.

RESULTS

Synthesis, properties and photobleaching of ACS769F4

A nonionic porphyrin derivative was synthesized by a three-step method based on our chlorosulfonation methodology (21). The one-pot mixed aldehyde–pyrrole condensation with nitrobenzene as oxidant, originated a mixture of the symmetric porphyrin 1 and the nonsymmetric porphyrin 2 (Fig. 1). The phenyl ring showed a higher reactivity than the 2,6-dichlorophenyl ring, allowing the controlled chlorosulphonation reaction of that mixture and, therefore, the production of the chlorosulphonyl derivative 3. Finally, the reaction of porphyrin 3 with 1,6-hexanediamine originated the nonsymmetric, noncharged, hydrophobic porphyrin, termed as ACS769F4.

The absorption spectra of ACS769F4 in DMF (Fig. 2A), showed a typical porphyrinic Soret band at 422 nm and the additional low intensity Q bands (*ca* 515, 550, 590 and 650 nm) (22). In agreement with the literature (14), similar values were observed for $TTAP^{4+}$ (Soret band at 412 nm) (Fig. 2B). The photobleaching experiment (Fig. 2) was carried out using the irradiation setup described above (fluence rate of 9.35 mW cm^{-2}) and was analyzed by following the decrease of absorbance at the Soret band. Within the analyzed spectral region (350–650 nm), no other photosensitive molecule was

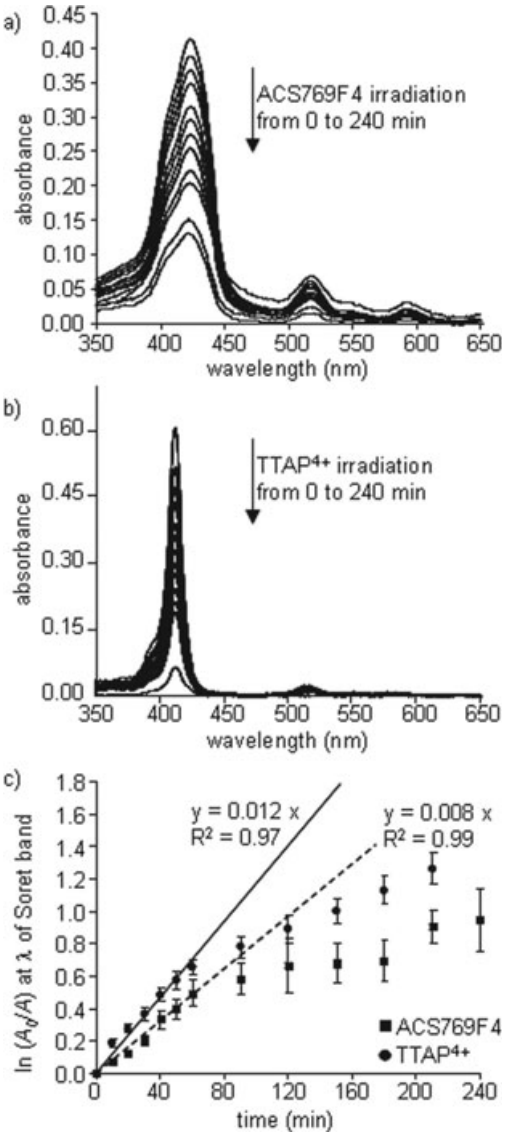

Figure 2. Photobleaching assays. UV–Visible absorption spectra variations upon exposure to visible light (9.35 mW cm^{-2}) of (A) ACS769F4 and (B) $TTAP^{4+}$ in DMF. (C) First-order plots for the first hour of photobleaching of ACS769F4 (■) and $TTAP^{4+}$ (●). Symbols and error bars are means ± SD of the values at each point, for three experiments.

produced by photodegradation of ACS769F4 or $TTAP^{4+}$, as no additional absorption peak was formed during irradiation (Fig 2A,B). In agreement with the literature (14), photobleaching reactions of both porphyrins showed first-order kinetics in the initial hour of exposure to light (Fig. 2C). Photo-degradation rate decay constants (k [min^{-1}]) and half-lifetimes ($t_{1/2}$ [min]), for ACS769F4 and $TTAP^{4+}$, were determined from their photobleaching first-order plots (Fig. 2C). Accordingly, a lower photodegradation rate decay constant ($k_{ACS769F4} = 0.8 \times 10^{-2}$ min^{-1}) and, consequently, a higher half-lifetime ($t_{1/2\ ACS769F4} = 86.6$ min) were observed for ACS769F4, compared with $TTAP^{4+}$ ($k_{\ TTAP4+} = 1.17 \times 10^{-2}$ min^{-1} and $t_{1/2\ TTAP4+} = 59.2$ min). The broader shape of the Soret band of ACS769F4 is indicative of some self-aggregation (14). The presence of chlorine atoms in the structure of ACS769F4 allows the increase of the singlet quantum yield of $^1O_2$ by the heavy atom effect (23) and the stability of the porphyrin. Although different environmental conditions are expected in biological systems (24) these are important properties for a photosensitizer.

Photoinactivation and dark-inactivation of bacteria

In order to determine and compare the antibacterial effects of both porphyrins, suspensions of *E. coli* (ATCC 25922 strain) and of *S. aureus* (ATCC 25923 strain), in PBS, were treated with different concentrations of ACS769F4 and $TTAP^{4+}$, from 1 to 15 μM. After dark incubation for 30 min at 37°C, cells were exposed to light for 15 min (8.4 J cm^{-2}) and 10-fold serial dilutions were then plated. Bacteria viability was assessed by counting the number of CFUs formed after 16 h at 37°C in the dark (Fig. 3). The effect of the light dose on the survival of bacteria after PDI treatment was evaluated (data not shown), becoming clear that a minimum of 15 min of light exposure (8.4 J cm^{-2}) is required to cause a significant reduction in bacteria survival. Viability of bacteria was not affected by this light dose without prior treatment with sensitizers or by incubation with solvent alone. A significantly ($P < 0.05$) higher PDI effect was observed for $TTAP^{4+}$ since dark incubation with a 1 μM solution of this sensitizer, followed by irradiation, caused a 4.6 $\log_{10}$ reduction in the viability of both *E. coli* and *S. aureus*. In contrast, 15 μM of ACS769F4 were required to reach 1.6 $\log_{10}$ and 3.0 $\log_{10}$ of photoinactivation of *E. coli* and *S. aureus*, respectively (Fig. 3), indicating a higher sensitivity of the latter strain to PDI treatment with this novel noncharged porphyrin.

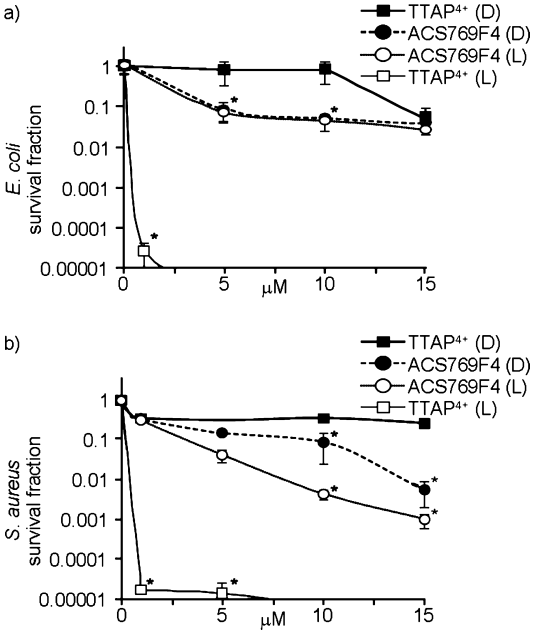

Figure 3. Dose-dependent toxicity of sensitizers in prokaryotic cells, *Escherichia coli* (A) and *Staphylococcus aureus* (B). (D) dark experiment; (L) irradiated experiment (see experimental). Symbols and error bars are means ± SD of the values at each point for three experiments.

Interesting was the performance of ACS769F4 in our experiments. They revealed that light exposure has only a small additional effect on the toxicity, since the survival curves of both bacterial strains incubated in the dark with this sensitizer were similar to those obtained from PDI experiments. Indeed, dark incubation with 15 μM of ACS769F4 caused a reduction in the viability of *S. aureus* and *E. coli* of 2.3 $\log_{10}$ and 1.4 $\log_{10}$, respectively. This effect was not observed for $TTAP^{4+}$, a statistically significant ($P < 0.05$) difference having been registered between the survival curves of dark incubation and PDI treatment with this sensitizer at concentrations above 1 μM. Moreover, dark incubation with ACS769F4 at concentrations below 15 μM was shown to have a significantly ($P < 0.05$) greater bactericidal effect than the dark incubation with $TTAP^{4+}$ at the same concentrations. Indeed, in the absence of light, $TTAP^{4+}$ caused less than 0.5 $\log_{10}$ reductions in the number of survivors of *S. aureus* and *E. coli* (Fig. 3).

As mentioned before, the cellular distribution of a sensitizer and, consequently, its interaction with surrounding biomolecules influences its toxicity during PDI (8). Therefore, to better understand the bactericidal effect of each sensitizer, we assessed their distribution within the bacterial cells by fluorescence microscopy. This was performed taking advantage of the red fluorescence (detected with the filter set-05) emitted by ACS769F4 and $TTAP^{4+}$, upon excitation at 412 and 422 nm, respectively.

After 1 h incubation of *E. coli* and *S. aureus* with ACS769F4, red fluorescence was detected only in aggregates, apparently located externally to the cells (Fig. 4A,E, respectively). Indeed, red fluorescence did not colocalize at each bacterial cell but, instead, appeared to be concentrated over the cells. Corroborating this observation, in such conditions, bacterial cells stained green (more visible in the panel E of Fig. 4), which may result from a reflection of the red fluorescence of the externally located sensitizer, as no green bacterial autofluorescence was detected. On the other hand, our data suggests that $TTAP^{4+}$ is internalized by both Gram-negative and Gram-positive bacteria (Fig. 4C,G, respectively). Control images showed no red autofluorescence in the bacterial cells. From these studies and in addition to those previously described (15,19,25), we believe that the strong phototoxicity of $TTAP^{4+}$ results from its intracellular localization. On the other hand, the significant toxicity observed for ACS769F4 may be justified by the presence of a long alkyl chain with a terminal amino group which can be protonated at cellular medium. This structure can interact with the lipophylic cell wall and cause some disturbance that allows bacteria

destruction with an activity similar to that observed for sphingosine (26).

Mammalian cell sensitivity to ACS769F4 and $TTAP^{4+}$

An important issue to be considered for clinical use is the potential toxicity of an antibacterial agent against the healthy surrounding tissues. Therefore, the phototoxicity of ACS 769F4 and $TTAP^{4+}$, their uptake, their intracellular distribution and their impact on the cytoskeleton of mammalian cells were evaluated using the HEK and BHK-21 cell lines. These cellular models, widely used in cellular biology research, are easily maintained in culture and give reproducible results, being appropriate for the present study. After incubation for 30 min in the dark with different concentrations of both sensitizers, in a range from 1 to 20 μM, cells were irradiated for 15 or 40 min (light dose of 8.4 and 22.4 J cm^{-2}, respectively) or, alternatively, kept in the dark for the same time. Cell viability was immediately assessed by the MTT assay, in order to understand the magnitude of toxicity of these treatments. Dark incubation for 70 min caused no reduction in the viability of mammalian cells, even at concentrations of porphyrin as high as 20 μM, indicating a lower susceptibility of either HEK (Fig. 5A) or BHK-21 (Fig. 5B) cells, to both sensitizers. Moreover, in the subsequent 96 h after treatment, mammalian cells continued to proliferate in a similar manner to nontreated cells (data not shown), proving their viability. With the same light dose used in bacteria experiments (8.4 J cm^{-2}) we did not observe any phototoxicity to the two lines of mammalian cells. Higher doses of light (22.4 J cm^{-2}) were required to cause some phototoxicity to mammalian cellular models. The two tested porphyrins seem to affect the two line cells in similar ways (Fig. 5). For HEK we observed a little more susceptibility for $TTAP^{4+}$ than for ACS769F4 and the contrary was observed in the case of BHK-21 cells. Control experiments showed that irradiation in the absence of sensitizers, and incubation with solvent, were harmless to mammalian cells.

Despite the relatively low toxicity observed of both sensitizers, ACS769F4 and $TTAP^{4+}$, for mammalian cells, it was important to assess where these molecules were internalized and

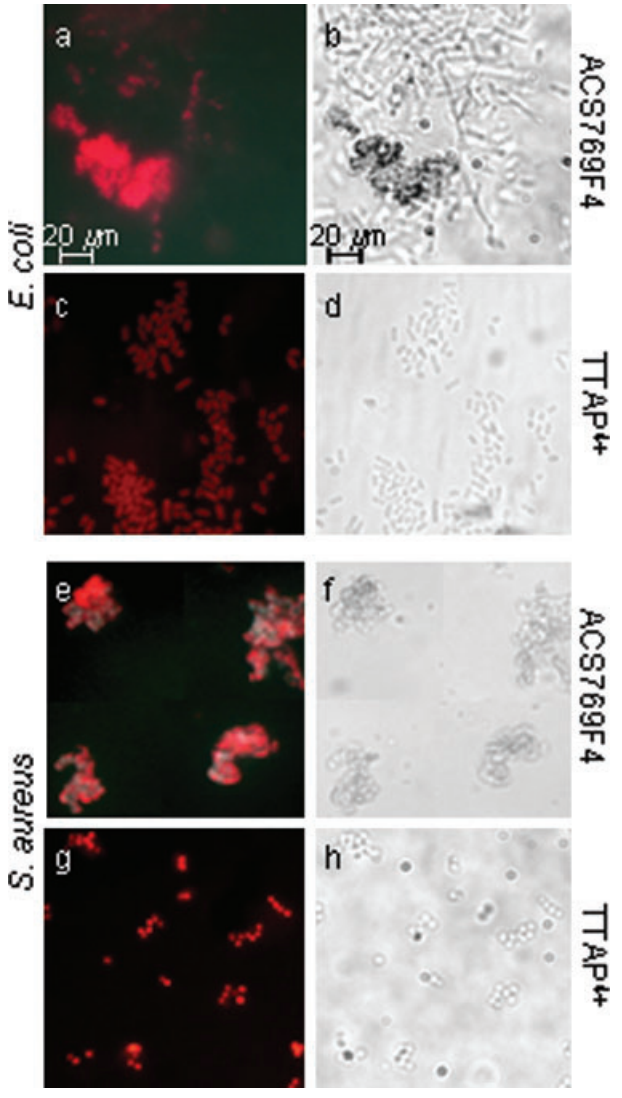

Figure 4. Evaluation of the external/internal accumulation of sensitizers in bacterial cells. Bacterial cells collected from a fresh culture, grown up until stationary phase, were incubated with 10 μM of ACS769F4 (red staining) or 5 μM of $TTAP^{4+}$ (red staining), for 1 h in the dark. (A, B) *Escherichia coli* with ACS769F4; (C, D) *E. coli* with $TTAP^{4+}$; (E, F) *Staphylococcus aureus* with ACS769F4; (G, H) *S. aureus* with $TTAP^{4+}$. Panels B, D, F and H correspond to the same image of panels A, C, E and G, respectively, observed by light microscopy. Bar: 20 μm.

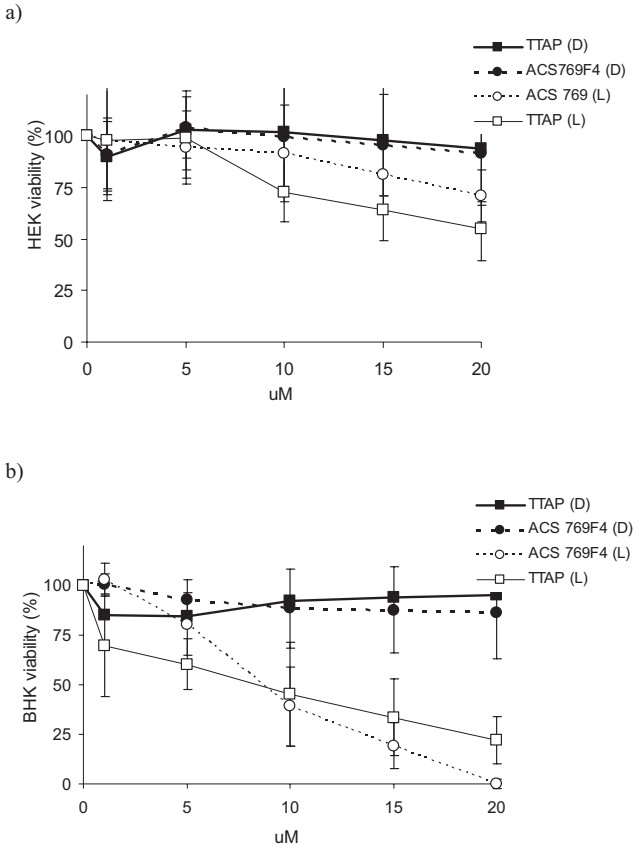

Figure 5. Dose-dependent toxicity of sensitizers in mammalian HEK (A) and BHK-21 (B) cell lines. (D) dark experiment; (L) irradiated experiment (see experimental). Symbols and error bars are means ± SD of the values at each point for six experiments.

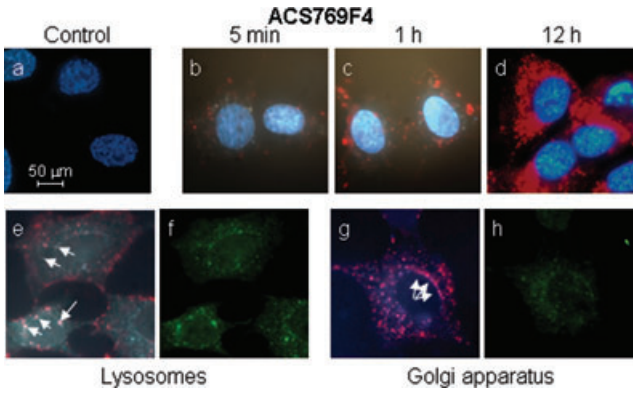

Figure 6. Intracellular distribution of ACF769F4 in mammalian cells. (A) BHK-21 cells (control without sensitizer). (B), (C) and (D), cells incubated with 10 μM of ACS769F4 in the dark at 37°C for 5 min, 1 h and 12 h, respectively. (E) and (G), dark incubation with the sensitizer for 1 h followed by immunodetection of the rab7 protein (1:1000 anti-Rab7 mAb) for lysosomes staining and of the 58K proteins/formimino-transferase cyclodeaminase (1:1000 anti-Golgi mAb) for Golgi staining, respectively. Images taken with the filter set-05: ACS769F4 in red (B, C, D, E and G); DAPI in blue, for nuclei staining (A, B, C and D); and fluorescein in white blue (E and G). White arrows show colocalization of ACS769F4 and both rab7 (E) and Golgi proteins (G). (F) and (H) correspond to the same image of (E) and (G), respectively, but taken with the filter set-10 (fluorescein in green). White bar: 50 μm.

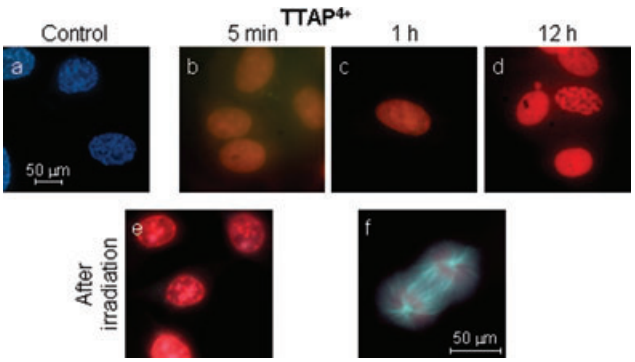

Figure 7. Intracellular distribution of $TTAP^{4+}$ in mammalian cells (A) BHK-21 cells (control without sensitizer). (B), (C) and (D), cells incubated with 10 μM of $TTAP^{4+}$ in the dark at 37°C for 5 min, 1 h and 12 h, respectively. (E) and (F), dark incubation with the sensitizer for 1 h followed by 40 min of irradiation (22.4 J cm^{-2}) or by immunodetection of microtubules' tubulin (1:1000 antitubulin mAb), respectively. Images taken with the filter set-05: $TTAP^{4+}$ in red (B, C, D, E and F); DAPI in blue, for nuclei staining (A); and fluorescein in white blue (F). White bar: 50 μm.

accumulated. Figure 6 shows BHK-21 cells, which do not exhibit autofluorescence (Fig. 6A), incubated with ACS769F4 at different time points. After 5 min of incubation, ACS769F4 was detected as dotted red fluorescence throughout the cell cytoplasm (Fig. 6B). Internalization of ACS769F4 should occur quite rapidly as, at this time point, we were not able to detect cytoplasmic membrane staining. No fluorescence was found in the nucleus of the cells, lowering the probabilities of genotoxicity. Longer incubation led to intracellular accumulation of additional ACS769F4 (Fig. 6C,D). Cell membrane permeabilization with TritonX-100 led to the loss of most intracellular ACS769F4, together with the cytosolic fraction (data not shown), suggesting that this sensitizer was mainly distributed through the cytosol. Additionally, ACS769F4 was found to be accumulated in vesicle-like structures, some of which colocalized with protein Rab-7, a lysosomal marker (white arrows in Fig. 6E) and with proteins from the Golgi complex (white arrows in Fig. 6G). These observations lead us to think that ACS769F4 may follow the pathway described for other sensitizers (20), which are internalized by endocytosis and accumulate in early and late endosomes and finally in lysosomes for degradation. Alternatively, once in the early endosomes, ACS769F4 may follow the classical secretion pathway through the Golgi apparatus. Further work should be done in order to clarify whether those spots of ACS769F4 that remained intracellularly after treatment with TritonX-100, and that did not colocalize with lysosomes or Golgi, were accumulated within endosomes. As demonstrated before (Fig. 4), due to its hydrophobicity, ACS769F4 form aggregates that may interfere with the ability to cross membranes. Therefore, it is expected that ACS769F4 should be internalized by pinocytosis and/or endocytosis, a feature that is not shared by bacteria.

In contrast, 5 min of incubation with $TTAP^{4+}$ revealed a faint fluorescence in the cytoplasm of the cell and its preferential accumulation in the nucleus (Fig. 7B), an effect that was even more pronounced after longer periods of incubation (Fig. 7C,D). $TTAP^{4+}$ was found to be directly associated with nuclear DNA, colocalizing with condensed chromosomes during mitosis (Fig. 7F). Its unusual cellular distribution pattern and its affinity for DNA raise doubts about the genotoxicity of $TTAP^{4+}$. Consistent with this, it became clear that irradiation in the presence of this sensitizer caused condensation of chromatin (Fig. 7E).

As the cellular integrity is dependent on the cytoskeleton organization, the toxicity of sensitizers was further assessed evaluating by immunodetection of tubulin and actin filaments the fate of microtubule and microfilament networks of BHK-21 cells. Our results indicated that incubation with 10 μM of ACS769F4 in the dark for 1 h did not disturb the microtubule (Fig. 8B) or the microfilament (Fig. 8H) networks, compared to controls (Fig. 8A,G, respectively). Furthermore, no alterations in the microtubule network were observed for cells incubated with 10 μM of ACS769F4 and then irradiated for 40 min (22.4 J cm^{-2}) (Fig. 8E in comparison to D). The microfilament network was disturbed by light exposure alone (Fig. 8J), becoming more concentrated around the nucleus, but this was not enhanced by incubation with 10 μM of ACS769F4 (Fig. 8K). We concluded that, in contrast to other sensitizers, that once released from lysosomes or endosomes cause cytoskeleton's photodamage (20), ACS769F4 was harmless to tubulin and actin networks.

On the other hand, BHK-21 cells incubated in the dark with 10 μM of $TTAP^{4+}$ (Fig. 8C in comparison to A) showed some level of disturbance in their microtubule network, which became less regular and less sharp, although at a level that did not compromise the mitotic spindle formation (Fig. 7F). A greater level of depolymerization was achieved after 40 min of exposure to light (22.4 J cm^{-2}) (Fig. 8F in comparison to D), which clearly shows that $TTAP^{4+}$ disturbs the integrity of the cell. However, no significant alterations were observed in the microfilament network after incubation with 10 μM of $TTAP^{4+}$, either in the dark (Fig. 8I) or after 40 min of irradiation (Fig. 8L) when compared to respective controls (Fig. 8G,J, respectively).

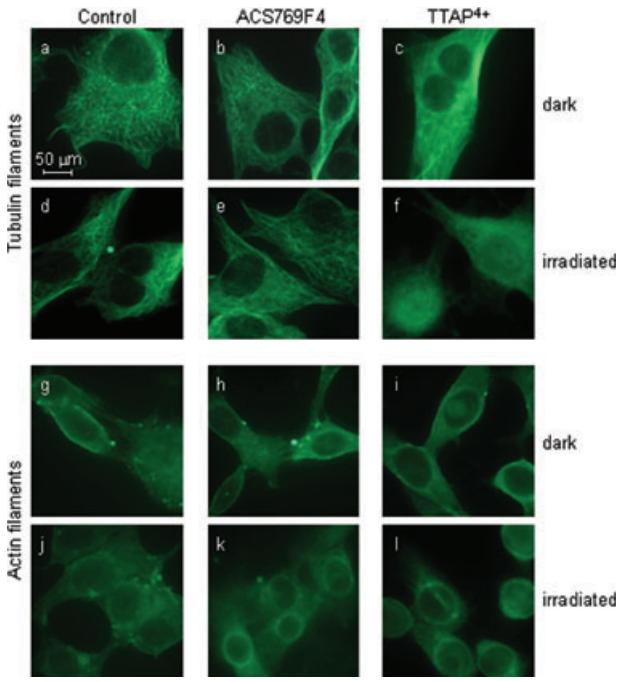

Figure 8. Impact of sensitizers in the cell cytoskeleton. BHK-21 cells incubated with 10 μM of ACS769F4 or of $TTAP^{4+}$ for 1 h in the dark at 37°C were irradiated for 40 min (22.4 J cm^{-2}) or were kept in the dark for control. Microtubules (panels A, B, C, D, E and F) and microfilaments (panels G, H, I, J, K and L) were immunostained with antitubulin mAb (1:1000) and with antiactin mAb (1:1000), respectively. (A, G) control without sensitizers, in the dark; (B, H) ACS769F4, in the dark; (C, I) $TTAP^{4+}$, in the dark; (D, J) control without sensitizers, with light exposure; (E, K) ACS769F4, with light exposure; (F, L) $TTAP^{4+}$, with light exposure. Images taken with the filter set-10 (fluorescein in green). White bar: 50 μm.

DISCUSSION

Antimicrobial PDT is a very promising alternative to antibiotics to eradicate bacteria in local infections (8). In the absence of structural features that turn sensitizers specific to bacteria, the challenge of antimicrobial PDT is to find molecules that efficiently eradicate bacteria without damage the host cells. The photophysical properties of sensitizers such as photostability and $^1O_2$ yields are crucial for the PDT event but intracellular distribution of molecules is also very important (13) due to the restricted radius of action and the extremely short lifetimes of the high-energy species produced (27). The cellular distribution of a sensitizer is determined by its structure and charge which influence the sensitizer hydrophilicity and aggregation state (19). Cationic porphyrins are among the most efficient sensitizers for antimicrobial PDT. The electrostatic interaction between these sensitizers and the negative charges on the outer surface of bacterial cells, allows their penetration to the inner plasma membrane of bacteria, most likely through the self-promoted uptake pathway, thereby enhancing their PDI effect (8,13–17,19,28). Differences in the mechanism of interaction of porphyrins with bacteria and mammalian cells are not difficult to accept given the structural differences between the cell walls of the former and the cytoplasmic membranes of the latter. It is thought that both amphiphilic cationic porphyrins (mono and dicationic) and the more hydrophilic ones (tri and tetracationic), are internalized by endocytosis, being accumulated afterward in lysosomes (29). The charged porphyrins acting as lipophylic cations, are targeted to the mitochondria, encouraged by the transmembrane potential of this organelle (29–31). In both cases, apoptotic cell death is induced upon exposure to light. Sensitizers in general do not accumulate in the nucleus of the mammalian cells and, when that happens, the risk of DNA damage, mutations and carcinogenesis increases (20,27). However, cationic sensitizers are known to have a high affinity for nucleic acids, showing an enhanced ability to induce DNA photodamage (32), inhibition of telomerase (33) and impairment of the topoisomerases activities (32–34). Therefore, the use of cationic porphyrins, which accumulate in the nucleus of mammalian cells, has as the biggest problem for the surrounding tissues the possibility of developing genotoxic effects. In the search for an efficient bactericidal sensitizer, harmless to mammalian cells, a novel nonionic porphyrin, ACS769F4 was synthesized. Its structure was modeled to have chlorine atoms in an appropriate place in order to improve the quantum yield of $^1O_2$ (21), and a long alkyl chain to favor the penetration into biological membranes as shown by others (8,17). All studies were carried out in comparison with $TTAP^{4+}$, a cationic porphyrin known for its efficiency in eradicating *E. coli* cellular suspensions (14,15). Both ACS769F4 and $TTAP^{4+}$ showed the typical absorption spectrum, with a Soret band at 422 and 412 nm, respectively. The broader shape of the Soret band of ACS769F4 is indicative of self aggregation (14), an undesirable property that may lead to a lower photosensitizing efficiency, since only monomeric species are appreciably photoactive (35). The noncationic porphyrin ACS769F4 showed a lower decay rate constant and, therefore, a longer half-life ($k_{ACS769F4} = 0.8 \times 10^{-2}$ min^{-1} and $t_{1/2\ ACS769F4} = 86.6$ min) during the first hour of the photobleaching reaction compared with those of $TTAP^{4+}$ ($k_{\ TTAP4+} = 1.17 \times 10^{-2}$ min^{-1} and $t_{1/2\ TTAP4+} = 59.2$ min). As is fairly well known, the photophysical properties measured in homogenous solution may differ from those in a biological environment (15,24). Indeed, porphyrins with similar photophysical properties, presented different antimicrobial phototoxicity based on differences in their cellular distribution and intrinsic photoactivity (13). In our case, $TTAP^{4+}$ was found to be more photoactive, since the treatment with just 1 μM of this sensitizer, followed by light exposure (8.4 J cm^{-2}), was sufficient for 99.999% bacterial killing (reduction of 4.6 $\log_{10}$) of both *E. coli* and *S. aureus*. By using higher doses of ACS769F4 (15 μM for *S. aureus* and 25 μM for *E. coli*), it was also possible to cause a 3 $\log_{10}$ reduction of bacteria after PDI treatment, achieving the recommended killing efficiency of 99.9% (36). In agreement with published data (13,16,28), *S. aureus* presented a higher photosusceptibility to both porphyrins than *E. coli*. However, significant improvements were achieved with ACS769F4 compared to other nonionic porphyrins described in the literature, since it presented an efficient PDI effect against Gram-negative bacteria, even without changing the permeability of the outer membrane of these (13,17,25). More studies are needed to assess whether administration of ACS769F4 with polycationic liposomes (37) or with bacterial outer membrane disrupting agents (*i.e.* $CaCl_2$, EDTA or polymixin B) (8) potentiates the PDI effect of this sensitizer. Another important consideration is that, while we were working with high cell density cultures

(10^8 cells mL^{-1}), some authors claim that PDI becomes more effective as the cell density decreases (38), suggesting that (photo)toxicity of both ACS769F4 and $TTAP^{4+}$ could be enhanced in bacterial cultures of lower density.

Interestingly, we found that with our experimental conditions, ACS769F4 also behaves as an effective bactericidal agent in the absence of light. Indeed, the PDI-toxicity dose-dependent curve of ACS769F4, in either *E. coli* or *S. aureus*, was slightly sharper than its dark-toxicity dose-dependent curve. Therefore, dark incubation of *S. aureus* and *E. coli* with 15 μM of ACS769F4 lead to a reduction of 2.3 $\log_{10}$ (99.5%) and of 1.4 $\log_{10}$ (93%) in the number of survivors, respectively. This fact is more relevant if we consider that the tested mammalian cell lines (HEK and BHK-21 cells) showed a very low dark-sensitivity for ACS769F4, even at concentrations as high as 20 μM. Also this is suggestive that the killing efficiency of this bactericidal agent can be improved by increasing the amount of light delivered. Dark toxicity was already described for some cationic porphyrin derivatives (39), however, to the best of our knowledge, side effects resulting for their use in mammalian cells are not known. More studies should be conducted to determine the dark-susceptibility to ACS769F4 in methicillin resistant *S. aureus* strains as, being the major cause of healthcare-associated infections, new methods to control and prevent their spread are urgently required (40).

Our data from fluorescence microscopy analyses suggested an influx of $TTAP^{4+}$ into bacterial cells. Further supporting this observation, Caminos and coworkers reported the ability of $TTAP^{4+}$ to tightly bind to *E. coli* cells (15). This was determined by measuring the fluorescence of the sensitizer in cell lysates, obtained from bacteria previously incubated with $TTAP^{4+}$ in the dark and washed immediately before lyses (15). In addition, Salmon-Divon *et al.* reported that the bactericidal effect of tetracationic porphyrins on *E. coli* is primarily dependent on genomic DNA photodamage (25). The suggested uptake of $TTAP^{4+}$ by bacterial cells may be justified by the electrostatic attraction to DNA (19). On the other hand, our data suggests that ACS769F4 forms aggregates on the external surface of the bacteria. As described for other sensitizers (19), this aggregation is probably due to its hydrophobicity and may potentiate the affinity of ACS769F4 for lipid membranes, while not allowing it to cross them. In fact, we are convinced that the long alkyl chain of the ACS769F4 acts as a hydrophobic arm, which penetrates deeply into the bacterial wall potentiating the PDI effect of the monomeric forms of this sensitizer.

Both prokaryotic and mammalian cells are known to be susceptible to photodynamic treatment and this is an important subject if a clinical application is expected. The HEK and BHK-21 mammalian cell lines showed a very low dark-sensitivity for either ACS769F4 or $TTAP^{4+}$. Indeed, we found that cells treated in the dark for 1 h with 20 μM of any of those sensitizers, continued to proliferate in a similar manner to nontreated cells, during the subsequent 96 h (data not shown). At this concentration, exposure to light pledged the mammalian cell viability. Nonetheless, it took a higher dose of light (*i.e.* 22.4 J cm^{-2}), than that used in bactericidal conditions (8.4 J cm^{-2}), to cause a significant reduction in their viability. In this case $TTAP^{4+}$ proved to be more damaging than ACS769F4 for HEK cells.

The accumulation of porphyrins was analyzed by fluorescence microscopy and showed that ACS769F4 and $TTAP^{4+}$ accumulate in different compartments of the cell in a time-dependent manner. In both cell lines ACS769F4 showed spotty fluorescence signals throughout the cytoplasm, part colocalizing with lysosomes and Golgi apparatus and most with the cytosolic fraction. The hydrophobicity properties of monomeric ACS769F4 enhanced by its long alkyl chain, favor the affinity toward lipid membranes. Therefore, after diffusion through the cytoplasmic membrane, ACS769F4 may bind to cytosolic proteins, insuring its solubilization. On the other hand, aggregated forms of ACS769F4 are expected to be internalized by endocytosis (20), justifying their accumulation in lysosomes (41). Sensitizers with this pattern of intracellular distribution have been described as being unable to photoinduce nuclear DNA damage (42). Moreover, we found that despite this intracellular distribution and in contrast to other cytosolic dyes (20), ACS769F4 caused no visible deleterious effect on the cytoskeleton of mammalian cells, even upon irradiation.

A different situation was found for $TTAP^{4+}$ which rapidly accumulates in the nucleus of mammalian cells and associates with DNA, probably by electrostatic attraction. This finding supports the suggested $TTAP^{4+}$ uptake by bacterial cells. A similar situation was described for *meso*-tetrakis(*N*-methyl-4-pyridiniumyl)-porphyrin (TMPyP) (43), known intercalating agent that present a nuclease-like activity, even in the absence of light and oxygen (44). The structural features that allow TMPyP and $TTAP^{4+}$ to concentrate in the nucleus are not fully known but the molecule charge must be determinant. It has been suggested that after endocytosis, TMPyP localizes temporarily in lysosomes, causing a faint staining of the cytoplasm, as observed for $TTAP^{4+}$, being then rapidly relocalized to the nucleus. There is evidence that its translocation to the nucleus is mediated by nuclear proteins, following a nuclear transport pathway (45). It is still unknown whether the $TTAP^{4+}$/DNA association happens by intercalation, outside groove binding, or outside binding with porphyrin self-stacking, mechanisms described for other cationic porphyrins (19). Given the similarities between the $TTAP^{4+}$ and TMPyP in terms of their structure and cellular distribution, it is expected that the mechanisms used by one or the other are also similar. *Per se* this is a huge drawback for the use of $TTAP^{4+}$ in antimicrobial PDT, as even working in conditions that apparently do not undermine the viability of mammalian cells, *i.e.* 1 μM, followed for 15 min of light exposure, there is no guarantee on safety in terms of genotoxic effects. In fact, we found that dark incubation with 10 μM of $TTAP^{4+}$ causes a deleterious effect on the microtubule network. Moreover, after irradiation, $TTAP^{4+}$ remained in the nucleus leading to chromatin condensation and changes in the cytoskeleton of the cell. More plausible is the possibility of induction of apoptosis in response to DNA damage caused by $TTAP^{4+}$, an event that will necessarily influence the organization of the cytoskeleton (46). For this porphyrin the higher reduction of viability observed in the case of BHK cells may be due to this effect. Highlighting the similarities between $TTAP^{4+}$ and TMPyP, it was shown that after irradiation, TMPyP-containing cells lose their mitochondrial transmembrane potential, inducing apoptosis (43).

In conclusion, ACS769F4 is a novel nonionic porphyrin sensitizer which showed evident *in vitro* ability to inactivate *E. coli* and *S. aureus*. The results showed clear differences in sensitivity of prokaryotic and mammalian cells, in terms of concentration of the sensitizer, and in terms of the light dose required to cause cell death. These results justify their disclosure and make ACS769F4 a very promising sensitizer to be considered for clinical use as an antimicrobial agent. This is even more relevant taking into account the comparison with $TTAP^{4+}$ which was shown to localize in the nucleus of the tested mammalian cells with interactions with DNA, a situation with awful perspectives for a molecule intended to be applied in humans.

Acknowledgements—The authors wish to thank Professor F. Mendes (Nuclear and Technological Institute, Portugal) for the valuable advices for the immunocytochemistry assays, Professor M. D. Amaral (Centre of Human Genetics, National Institute of Health, Portugal) for the BHK-21 and HEK cell lines, Mr. Benjamin for the photometer (Konica Minolta AutoMeter IV F) used to measure the light dose of our irradiation setup at the beginning of the experiments, and finally Professor L. Clarke (Faculty of Sciences, University of Lisbon, Portugal) for revising the manuscript. This work was supported by "Cancer Light Assisted Receeding Oncologic" (CLARO) project grant (Agência de Inovação, Portugal). Both SM and FC were recipients of research fellowships from CLARO's grant (Portugal).

SUPPORTING INFORMATION

Additional Supporting Information may be found in the online version of this article:

Figure S1. NMR spectrum of ACS 769F4 (*TFA sinal).

Figure S2. IR spectrum of ACS 769F4: NH band at 3429 cm^{-1}; CH saturated at 2929 cm^{-1}; sulfonamide at 1159 cm^{-1}; porphyrin macocycle at 1557, 1428 and 803 cm^{-1}.

Figure S3. ESI spectrum of ACS 769F4.

Figure S4. Visible spectrum of ACS 769F4 (CH_2Cl_2/MeOH).

Please note: Wiley-Blackwell is not responsible for the content or functionality of any supporting information supplied by the authors. Any queries (other than missing material) should be directed to the corresponding author for the article.

REFERENCES

1. Plaetzer, K., B. Krammer, J. Berlanda, F. Berr and T. Kiesslich (2009) Photophysics and photochemistry of photodynamic therapy: Fundamental aspects. *Lasers Med. Sci.* **24**, 259–268.
2. Tao, J. N., S. M. Duan and J. Li (2007) Experimental studies on treatment of HSV infections with photodynamic therapy using 5-aminolevulinic acid. *Zhonghua Shi Yan He Lin Chuang Bing Du Xue Za Zhi* **21**, 79–82.
3. Hamblin, M. R. and T. Hasan (2004) Photodynamic therapy: A new antimicrobial approach to infectious disease? *Photochem. Photobiol. Sci.* **3**, 436–450.
4. Fuchs, B. B., G. P. Tegos, M. R. Hamblin and E. Mylonakis (2007) Susceptibility of *Cryptococcus neoformans* to photodynamic inactivation is associated with cell wall integrity. *Antimicrob. Agents Chemother.* **51**, 2929–2936.
5. Wagner, S. J., A. Skripchenko, J. Salata and L. J. Cardo (2007) Photoinactivation of *Trypanosoma cruzi* in red cell suspensions with thiopyrylium. *Transfus. Apher. Sci.* **37**, 23–25.
6. Maisch, T. (2007) Anti-microbial photodynamic therapy: Useful in the future? *Lasers Med. Sci.* **22**, 83–91.
7. Tang, H. M., M. R. Hamblin and C. M. Yow (2007) A comparative in vitro photoinactivation study of clinical isolates of multidrug-resistant pathogens. *J. Infect. Chemother.* **13**, 87–91.
8. Jori, G., C. Fabris, M. Soncin, S. Ferro, O. Coppellotti, D. Dei, L. Fantetti, G. Chiti and G. Roncucci (2006) Photodynamic therapy in the treatment of microbial infections: Basic principles and perspective applications. *Lasers Surg. Med.* **38**, 468–481.
9. Hamblin, M. R., D. A. O'Donnell, N. Murthy, C. H. Contag and T. Hasan (2002) Rapid control of wound infections by targeted photodynamic therapy monitored by in vivo bioluminescence imaging. *Photochem. Photobiol.* **75**, 51–57.
10. Lembo, A. J., R. A. Ganz, S. Sheth, D. Cave, C. Kelly, P. Levin, P. T. Kazlas, P. C. Baldwin III, W. R. Lindmark, J. R. McGrath and M. R. Hamblin (2009) Treatment of *Helicobacter pylori* infection with intra-gastric violet light phototherapy: A pilot clinical trial. *Lasers Surg. Med.* **41**, 337–344.
11. Garcez, A. S., M. S. Ribeiro, G. P. Tegos, S. C. Nunez, A. O. Jorge and M. R. Hamblin (2007) Antimicrobial photodynamic therapy combined with conventional endodontic treatment to eliminate root canal biofilm infection. *Lasers Surg. Med.* **39**, 59–66.
12. Garcez, A. S., S. C. Nunez, M. R. Hamblin and M. S. Ribeiro (2008) Antimicrobial effects of photodynamic therapy on patients with necrotic pulps and periapical lesion. *J. Endod.* **34**, 138–142.
13. Merchat, M., G. Bertolini, P. Giacomini, A. Villanueva and G. Jori (1996) Meso-substituted cationic porphyrins as efficient photosensitizers of gram-positive and gram-negative bacteria. *J. Photochem. Photobiol. B* **32**, 153–157.
14. Caminos, D. A. and E. N. Durantini (2006) Photodynamic inactivation of *Escherichia coli* immobilized on agar surfaces by a tricationic porphyrin. *Bioorg. Med. Chem.* **14**, 4253–4259.
15. Caminos, D. A., M. B. Spesia, P. Pons and E. N. Durantini (2008) Mechanisms of *Escherichia coli* photodynamic inactivation by an amphiphilic tricationic porphyrin and 5,10,15,20-tetra(4-N,N,N-trimethylammoniumphenyl) porphyrin. *Photochem. Photobiol. Sci.* **7**, 1071–1078.
16. Hamblin, M. R., D. A. O'Donnell, N. Murthy, K. Rajagopalan, N. Michaud, M. E. Sherwood and T. Hasan (2002) Polycationic photosensitizer conjugates: Effects of chain length and Gram classification on the photodynamic inactivation of bacteria. *J. Antimicrob. Chemother.* **49**, 941–951.
17. Alves, E., L. Costa, C. M. Carvalho, J. P. Tome, M. A. Faustino, M. G. Neves, A. C. Tome, J. A. Cavaleiro, A. Cunha and A. Almeida (2009) Charge effect on the photoinactivation of Gram-negative and Gram-positive bacteria by cationic meso-substituted porphyrins. *BMC Microbiol.* **9**, 70.
18. Caminos, D. A., M. B. Spesia and E. N. Durantini (2006) Photodynamic inactivation of *Escherichia coli* by novel meso-substituted porphyrins by 4-(3-N,N,N-trimethylammoniumpropoxy)phenyl and 4-(trifluoromethyl)phenyl groups. *Photochem. Photobiol. Sci.* **5**, 56–65.
19. Lang, K., J. Mosinger and D. M. Wagnerová (2004) Photophysical properties of porphyrinoid sensitizers non-covalently bound to host molecules; models for photodynamic therapy. *Coord. Chem. Rev.* **248**, 321–350.
20. Dougherty, T. J., C. J. Gomer, B. W. Henderson, G. Jori, D. Kessel, M. Korbelik, J. Moan and Q. Peng (1998) Photodynamic therapy. *J. Natl Cancer Inst.* **90**, 889–905.
21. Ribeiro, S. M., A. C. Serra and A. M. d. Rocha-Golsaves (2007) Covalently immobilized porphyrins as photooxidation catalysts. *Tetrahedron* **63**, 7885–7891.
22. Barnett, G. H., M. F. Hudson and K. M. Smith (1975) Concerning meso-tetraphenylporphyrin purification. *J. Chem. Soc.* **14**, 1401–1403.
23. Azenha, E. G., A. C. Serra, M. Pineiro, M. M. Pereira, J. Seixas de Melo, L. G. Arnaut, S. J. Formosinho and A. M. d' A. Gonsalves (2002) Heavy-atom effects on metalloporphyrins and polyhalogenated porphyrins. *Chem. Phys.* **280**, 177–190.
24. Bezdetnaya, L., N. Zeghari, I. Belitchenko, M. Barberi-Heyob, J. L. Merlin, A. Potapenko and F. Guillemin (1996) Spectroscopic and biological testing of photobleaching of porphyrins in solutions. *Photochem. Photobiol.* **64**, 382–386.

25. Salmon-Divon, M., Y. Nitzan and Z. Malik (2004) Mechanistic aspects of *Escherichia coli* photodynamic inactivation by cationic tetra-meso(N-methylpyridyl)porphine. *Photochem. Photobiol. Sci.* **3**, 423–429.
26. Possemiers, S., J. Van Camp, S. Bolca and W. Verstraete (2005) Characterization of the bactericidal effect of dietary sphingosine and its activity under intestinal conditions. *Int. J. Food Microbiol.* **105**, 59–70.
27. Sobolev, A. S., D. A. Jans and A. A. Rosenkranz (2000) Targeted intracellular delivery of photosensitizers. *Prog. Biophys. Mol. Biol.* **73**, 51–90.
28. Maisch, T., C. Bosl, R. M. Szeimies, N. Lehn and C. Abels (2005) Photodynamic effects of novel XF porphyrin derivatives on prokaryotic and eukaryotic cells. *Antimicrob. Agents Chemother.* **49**, 1542–1552.
29. Mroz, P., J. Bhaumik, D. K. Dogutan, Z. Aly, Z. Kamal, L. Khalid, H. L. Kee, D. F. Bocian, D. Holten, J. S. Lindsey and M. R. Hamblin (2009) Imidazole metalloporphyrins as photosensitizers for photodynamic therapy: Role of molecular charge, central metal and hydroxyl radical production. *Cancer Lett.* **282**, 63–76.
30. Lei, W., J. Xie, Y. Hou, G. Jiang, H. Zhang, P. Wang, X. Wang and B. Zhang (2010) Mitochondria-targeting properties and photodynamic activities of porphyrin derivatives bearing cationic pendant. *J. Photochem. Photobiol. B* **98**, 167–171.
31. Ngen, E. J., P. Rajaputra and Y. You (2009) Evaluation of delocalized lipophilic cationic dyes as delivery vehicles for photosensitizers to mitochondria. *Bioorg. Med. Chem.* **17**, 6631–6640.
32. Munson, B. R. and R. J. Fiel (1992) DNA intercalation and photosensitization by cationic meso substituted porphyrins. *Nucleic Acids Res.* **20**, 1315–1319.
33. Dixon, I. M., F. Lopez, J. P. Esteve, A. M. Tejera, M. A. Blasco, G. Pratviel and B. Meunier (2005) Porphyrin derivatives for telomere binding and telomerase inhibition. *Chembiochem.* **6**, 123–132.
34. Shuai, L., S. Wang, L. Zhang, B. Fu and X. Zhou (2009) Cationic porphyrins and analogues as new DNA topoisomerase I and II inhibitors. *Chem. Biodivers.* **6**, 827–837.
35. Ball, D. J., S. R. Wood, D. I. Vernon, J. Griffiths, T. M. Dubbelman and S. B. Brown (1998) The characterisation of three substituted zinc phthalocyanines of differing charge for use in photodynamic therapy. A comparative study of their aggregation and photosensitising ability in relation to mTHPC and polyhaematoporphyrin. *J. Photochem. Photobiol. B* **45**, 28–35.
36. Boyce, J. M. and D. Pittet (2002) Guideline for hand hygiene in health-care settings. Recommendations of the Healthcare Infection Control Practices Advisory Committee and the HIPAC/SHEA/APIC/IDSA Hand Hygiene Task Force. *Am. J. Infect. Control* **30**, S1–S46.
37. Ferro, S., F. Ricchelli, D. Monti, G. Mancini and G. Jori (2007) Efficient photoinactivation of methicillin-resistant *Staphylococcus aureus* by a novel porphyrin incorporated into a poly-cationic liposome. *Int. J. Biochem. Cell Biol.* **39**, 1026–1034.
38. Demidova, T. N. and M. R. Hamblin (2005) Effect of cell-photosensitizer binding and cell density on microbial photoinactivation. *Antimicrob. Agents Chemother.* **49**, 2329–2335.
39. Ooi, N., K. Miller, C. Randall, W. Rhys-Williams, W. Love and I. Chopra (2010) XF-70 and XF-73, novel antibacterial agents active against slow-growing and non-dividing cultures of *Staphylococcus aureus* including biofilms. *J. Antimicrob. Chemother.* **65**, 72–78.
40. Kurlenda, J., M. Grinholc, K. Jasek and G. Wegrzyn (2007) RAPD typing of methicillin-resistant *Staphylococcus aureus*: A 7-year experience in a Polish hospital. *Med. Sci. Monit.* **13**, MT13–MT18.
41. Bonneau, S., P. Morliere and D. Brault (2004) Dynamics of interactions of photosensitizers with lipoproteins and membrane-models: Correlation with cellular incorporation and subcellular distribution. *Biochem. Pharmacol.* **68**, 1443–1452.
42. Egyeki, M., K. Toth, W. Waldeck, P. Schmezer, J. Langowski and G. Csik (2006) DNA damaging capability of hematoporphyrin towards DNAs of various accessibilities. *J. Photochem. Photobiol. B* **84**, 119–127.
43. Hatz, S., J. D. Lambert and P. R. Ogilby (2007) Measuring the lifetime of singlet oxygen in a single cell: Addressing the issue of cell viability. *Photochem. Photobiol. Sci.* **6**, 1106–1116.
44. Meunier, B. (1992) Metalloporphyrins as versatile catalysts for oxidation reactions and oxidative DNA cleavage. *Chem. Rev.* **92**, 1411–1456.
45. Patito, I. A., C. Rothmann and Z. Malik (2001) Nuclear transport of photosensitizers during photosensitization and oxidative stress. *Biol. Cell* **93**, 285–291.
46. Bursch, W., A. Ellinger, C. Gerner, U. Frohwein and R. Schulte-Hermann (2000) Programmed cell death (PCD). Apoptosis, autophagic PCD, or others? *Ann. NY Acad. Sci.* **926**, 1–12.